Expression of Supramolecular Chirality in Aggregates of Chiral Amide-Containing Surfactants

N. A. J. M. Sommerdijk,* P. J. J. A. Buynsters, H. Akdemir, D. G. Geurts, A. M. A. Pistorius, M. C. Feiters, R. J. M. Nolte, and B. Zwanenburg

Abstract: The aggregation behaviour of a series of chiral amide-containing surfactants **1**–**5** is studied in order to assess the structural requirements for the generation of supramolecular chirality. It is found that the presence of hydrogen-bonding moieties (i.e., amide groups) in the molecules alone is not sufficient for the formation of chiral aggregates and that the expression of chirality at a higher level, for example in the form of helical structures, strongly depends on the head-group organisation of the surfactant molecules. By changing the intermolecular interactions between the molecules, for example by pH variation or metal-ion complexation, this head-group organisation can be tuned in such a way that supramolecular expression of chirality is induced or altered in the aggregates.

Keywords: aggregations · chirality · helical structures · hydrogen bonds · supramolecular chemistry · surfactants

Introduction

The construction of chiral supramolecular structures by the self-assembly of chiral surfactant molecules has received much attention in the last decade. Synthetic surfactants derived from sugars,[1] amino acids,[2] nucleic acids[3] and phospholipids[4] have been demonstrated to form a variety of chiral assemblies, such as helical fibres, twisted ribbons, etc. Other superstructures, such as rods and tubules, have also been generated from nonchiral surfactants.[5] Although the physical properties of these self-assembling systems have been extensively studied, little progress has been made in relating structures of the supramolecule to those of the constituent surfactants.[6]

Theoretical studies on tubule formation indicate that the creation of chiral superstructures is based on chiral interaction of individual molecules in the bilayer, and that the magnitude of this chirality, that is, the amount of twist in the molecular packing, determines the dimensions of the supramolecular structure.[7] Although the importance of hydrogen bonding in aggregation behaviour is well recognised,[8] little is known about the relationship between the structure of the molecules and the way they organise to form chiral aggregates. Frankel and O'Brien have compared electron microscopic information with predictions of hydrogen bond formation obtained from molecular modelling calculations for a large number of aldolamides.[9]

Here we report on the aggregation behaviour of a novel series of structurally related amide-containing surfactants **1**–**5,** which were synthesised with the objective of studying the factors determining the generation of chiral supramolecular aggregates.[10,11] These surfactants contain phosphate and imidazole moieties as head-groups whose size and orientation can be adjusted by means of protonation and metal-ion complexation. The effect of these modifications on the

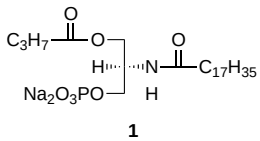

1

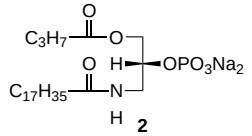

2

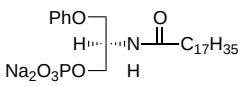

3

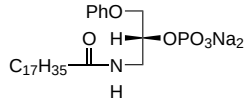

4

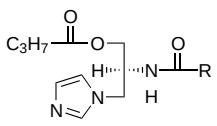

5a: R=$C_{17}H_{35}$
5b: R=$C_{11}H_{23}$

5

[*] Dr. N. A. J. M. Sommerdijk, P. J. J. A Buynsters, H. Akdemir, D. G. Geurts, Dr. M. C. Feiters, Prof. Dr. R. J. M. Nolte, Prof. Dr. B. Zwanenburg
Department of Organic Chemistry
NSR-Institute for Molecular Structure, Design and Synthesis
University of Nijmegen
Toernooiveld, 6525 ED Nijmegen (The Netherlands)
Fax: Int. code + 31 80 24365-2929
e-mail: nicos@sci.kun.nl

Dr. A. M. A. Pistorius
Department of Biochemistry, University of Nijmegen
Adelbertusplein 1, Nijmegen (The Netherlands)

  0947-6539/98/0401-0127 $ 17.50+.25/0

Table 1. Physical data for aggregates of compounds **1**–**5a** prepared at pH 6.5.

Compound	DSC			d (Å) [a]	Molecular area (Å^2)	Lift-off area (Å^2)
	T_c (°C)	ΔH (J g^{-1})	ΔS (J g^{-1} K^{-1})			
1	16	5.2	0.02	40	125 (105 [b])	370 (250 [b])
2	29	960	3.14	46	38 (35 [b])	80 (74 [b])
3	21 (26 [b])	23 (40 [b])	0.08 (0.13 [b])	34 (45 [b])	56	81
4	– [c]	– [c]	–	40	– [c]	– [c]
5a	49	86	0.29	39	56	94
5a/$CuSO_4$	31	14	0.05	38	60	94
5a/$Cu(Trf)_2$	20	22	0.08	40	63	102

[a] Powder diffraction d spacing. [b] pH adjusted to 2.5. [c] Not observed.[33]

interactions between the molecules and on the supramolecular expression of chirality is presented. It will be shown that the supramolecular expression of chirality is directly linked to the head-group organisation in the surfactant molecules.

Results and Discussion

Aggregation behaviour of butyrates 1 and 2: Both **1** and **2** are obtained after reaction of the appropriate *N*-acylated aziridine with dibenzyl phosphate and subsequent debenzylation.[11] Compounds **1** and **2** have a strong structural resemblance but differ in the position of the phosphate and amide groups in the molecules. Both positional isomers have an (*R*) configuration. As shown below, their structural differences lead to a dramatic effect on the expression of chirality at the supramolecular level.

Transmission electron microscopy on samples prepared from aqueous 2% (w/w) dispersions demonstrated that **1** formed planar structures, whereas **2** produced left-handed helical strands which coagulated to form left-handed, ropelike structures (Figure 1a).[10] These helical strands have a diameter of 22 nm and a large, regular pitch of 92 nm. Since the coiled strands appear to be round, they probably have a tubular structure with a single or multibilayer wall. Powder diffraction experiments revealed a repetitive distance of 40 and 46 Å (Table 1) for cast films of the aggregates of **1** and **2**, respectively. These values indicate that the aggregates of both compounds are constructed from intercalated bilayers, since the maximum molecular length of both compounds, as estimated from CPK models, amounts to approximately 30 Å. The aggregates prepared from **1** displayed a weak phase transition at 16 °C, whereas those of **2** showed a remarkably strong transition at 29 °C (Table 1), indicating that **1** and **2** form aggregates with different types of hydrocarbon chain organisation (vide infra).

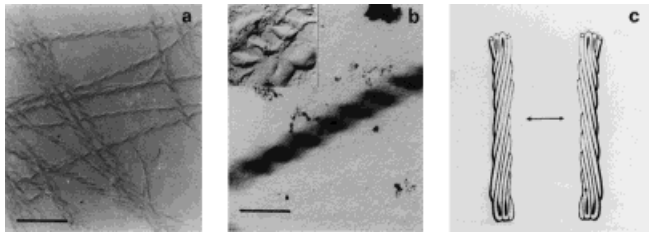

Figure 1. Electron micrographs taken from 2% (w/w) dispersions of **2** (pH 6.5, bars 500 nm): a) left-handed helices from **2** (Pt shadowing), b) right-handed superhelix from **2** (unstained; inset: freeze fracture); c) schematic representation of the model proposed for the chiral packing of DNA molecules by Reich et al. Each of the individual strands represents a double helix. (Taken from ref. [16].)

Aggregation experiments performed with the (*S*) enantiomers of **1** and **2** proved that the inversion of the stereocentre led to a reversal of the sense of supramolecular chirality, but did not affect the aggregation behaviour otherwise.

Monolayer experiments revealed another striking difference between **1** and **2**. A very large lift-off area of approximately 350 Å^2 was determined for **1** (Figure 2, Table 1) and no clear liquid condensed phase was observed upon compression. This feature may be explained by assuming that compound **1** has a molecular conformation as depicted in Figure 2, where both the amide hydrocarbon chain and the

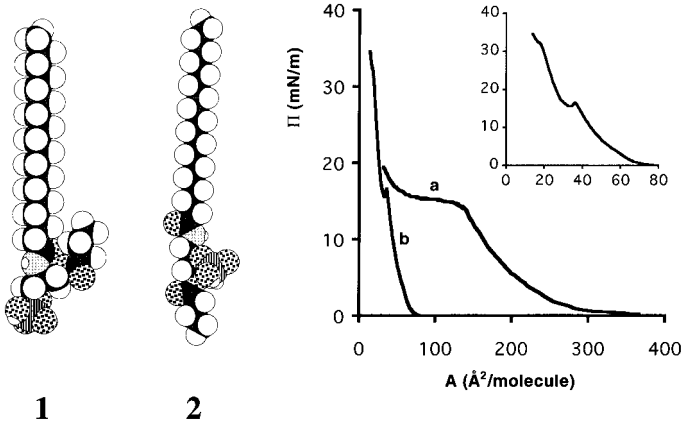

1 **2**

Figure 2. Proposed conformations of **1** and **2**, and monolayer isotherms of a) **1** and b) **2**, recorded on an aqueous subphase of pH 6. 5.at 20 °C. Inset: enlargement of the isotherm of **2**.

Abstract in Dutch: *Het aggregatiegedrag van een reeks surfactantmoleculen (**1**–**5**) die amidegroepen bevatten, is onderzocht met als doel het verkrijgen van inzicht in de voorwaarden die aan de structuur van een molecuul gesteld moeten worden om supramoleculaire chiraliteit te genereren. De aanwezigheid van groepen die waterstofbruggen kunnen vormen (amidegroepen) blijkt niet voldoende te zijn om chirale aggregaten te geven. Het tot uitdrukking brengen van chiraliteit op een hoger niveau, bijvoorbeeld in de vorm van helices, hangt sterk af van de organisatie van de kopgroepen van de surfactantmoleculen. Door de intermoleculaire interacties te veranderen, bijvoorbeeld door de pH te varieren of door het complexeren van metaalionen, kan de organisatie van de kopgroepen zodanig worden afgeregeld dat in de aggregaten de supramoleculaire chiraliteit tot uitdrukking komt of verandert.*

0947-6539/98/0401-0128 $ 17.50+.50/0 *Chem. Eur. J.* **1998**, *4*, No. 1

butyrate group point away from the subphase. In this arrangement the head-group area will be too large to allow efficient hydrocarbon chain packing, hence no condensed phase will be formed. Its positional isomer **2** could be compressed, however, to a much smaller area per molecule (80 Å^2) before an increase of surface pressure was observed (Figure 2). The observed low area per molecule suggests that **2** adopts a structure in which the butyrate group is immersed in the subphase as indicated in Figure 2.[10,12]

During compression, the monolayers were studied by Brewster angle microscopy.[13] Compound **1** did not show any distinct morphologies, whereas for monolayers of compound **2** the growth of chiral branched domains was observed (Figure 3a), which exhibited an overall counterclockwise

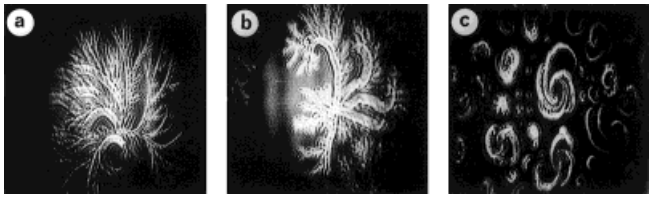

Figure 3. Brewster angle micrographs of surface monolayers of **2** (spot diameter 600 nm). a) pH 6.5, 30 °C, 16 mN m^{-1}; b) pH 6.5, 10 °C, 15 mN m^{-1}; c) pH 2.5, 20 °C, 15 mN m^{-1}.

pattern.[10,14] Upon compression into the liquid condensed (LC) phase the chirality of these domains was lost, due to the intercalation of the branches. The size and shape of the observed domains changed when the temperature of the subphase was decreased. At lower temperatures smaller domains were observed that showed a higher degree of curvature in the branches (Figure 3b).[15]

In addition to the left-handed helices described above, a small number of very large, right-handed helices were also observed in dispersions of **2** (Figure 1b). These superhelices had a thickness of 350 nm and a pitch of 250 nm. It is quite possible that these right-handed superhelices are composed of intertwined left-handed helices. A similar intertwined structure has been reported for supercoiled linear DNA (Figure 1c).[16] Minor changes in salt concentration, which are believed to induce modifications in the hydration state and in the surface charge density (or distribution) of the DNA molecules can affect the twist and lead to a reversal of the handedness of the supercoil. Thus supercoiling may lead to the formation of either left-handed or right-handed helical structures, regardless of the handedness of the individual strands. By analogy, it is proposed that in the present case small changes in local ion concentrations (e.g. pH, vide infra) may induce the formation of right-handed superhelices from the left-handed helices shown in Figure 1a.

In order to investigate the effect of pH on the formation of chiral domains, monolayer experiments were carried out at pH values at which the phosphate groups of **1** and **2** are fully protonated.[17] Isotherms recorded at pH = 2.5 revealed a decrease in molecular area for both surfactants, but for **1** the changes were more pronounced than for **2** (Table 1). No change in the morphology of the monolayer of **1** could be observed by Brewster angle microscopy, however. In contrast, the size of the domains in the monolayer of **2** decreased and their direction of growth was reversed (Figure 3c). This phenomenon is unprecedented and must be due to a change in molecular organisation of the surfactant molecules, leading to a different long-range tilt order in the domains.[18] This observed reversal of growth may arise from a reduction of the dipole–dipole repulsive interactions between the surfactant molecules, as well as from a reorganisation of the hydrogen bonding pattern.

Aggregation behaviour of phenyl ethers 3 and 4: With the aim of obtaining more information about its role in the generation of chiral superstructures[10] (vide infra), we replaced the ester group by an ether function. A phenoxy group was chosen due to the availability of enantiopure synthetic precursors.[11]

Electron microscopy demonstrated that vesicles with diameters of 500–1000 nm were generated when **3** was dispersed in water of pH 6.5 (2%, w/w). These vesicles slowly rearranged to form ribbons (Figure 4a) which displayed a phase tran-

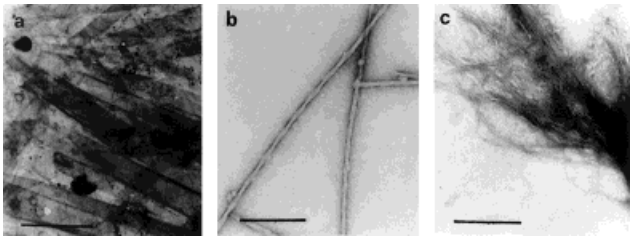

Figure 4. Electron micrographs of negatively stained samples from aqueous 2% (w/w) dispersions of **3** and **4**. a) Ribbons of **3** (pH 6.5, bar 1000 nm); b) helices of **3** (pH 2.5, bar 1000 nm); c) fibres of **4** (pH 6.5, bar 500 nm).

sition at 21 °C (Table 1). Powder diffraction revealed a bilayer thickness of 34 Å (Table 1), suggesting that the ribbons have a structure in which the alkyl chains are intercalating. The observed broadening of the d_s reflection[19] at 4.23 Å ($2\theta = 21.05°$) indicates that the packing of the alkyl chains is distorted; this can be attributed to a tilted orientation of the lipid molecules. The molecular area of 56 Å^2 deduced from monolayer experiments (Table 1) indicates that **3** adopts a conformation similar to that of **1**, with the phenoxy group pointing away from the aqueous phase.

Electron micrographs of samples prepared from aqueous 2% (w/w) dispersions of **4** revealed the presence of fibrous aggregates (Figure 4c). These fibres were formed immediately after preparation of the samples and remained stable for at least one week. Powder diffraction patterns obtained from cast films of **4** reveal higher order reflections from which a repetitive distance of 40 Å was derived (Table 1). This value suggests that these fibres are built up from intercalating building blocks composed of two molecules of **4**, probably forming a staircase-like arrangement (Figure 5).[20] This would yield a micellar fibre having a low degree of hydrocarbon chain organisation. This proposal is supported by the fact that no reflections of a hexagonal packing of alkyl chains were observed in the powder diffraction patterns and that DSC experiments did not show any phase transition.

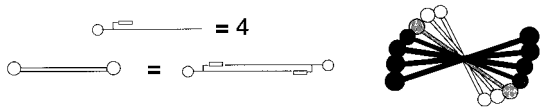

Figure 5. Schematic representation of the possible arrangement of the molecules of **4** in a micellar fibre.

It was found that protonation[21] of the head groups of **3** led to the formation of chiral aggregates from the ribbonlike structures which were initially present (Figure 4b). When the pH of an aqueous 2% (w/w) dispersion of **3** was lowered from pH 6.5 to 2.5 these ribbons started to twist. This twisting formed left-handed helices which, ultimately, transformed into tubular structures. For these chiral aggregates DSC experiments revealed a phase transition (Table 1) at 26°C, which is 5°C higher than the phase-transition temperature of the ribbons found at pH 6.5. This feature and the higher ΔH and ΔS values measured at pH 2.5 suggest that the molecules in the chiral tubular structures have a higher degree of molecular organisation than the molecules in the ribbons. Remarkably, the powder diffraction pattern indicated that upon changing the pH to 2.5, the bilayer thickness increased from 34 to 45 Å (Table 1). This may be explained by a decrease of the molecular tilt angle, or a lower degree of intercalation of the hydrocarbon chains. It was found that the change in bilayer thickness was accompanied by a sharpening of the d_s reflection, supporting the former explanation.[19]

Aggregation behaviour of imidazolyl surfactants 5: Electron microscopy performed on aqueous dispersions containing 0.1% (w/w) of **5a** revealed that this compound formed planar bilayer aggregates. These planar structures displayed a phase transition at 49°C (Table 1). Powder diffraction patterns obtained from cast films of **5a** showed higher order reflections from which a bilayer thickness of 39 Å was calculated (Table 1). The total molecular length of **5a** estimated from CPK models, is 28 Å, which suggests that the hydrocarbon chains of the molecules in the aggregates are intercalated.

When the length of the hydrocarbon chains in **5a** was reduced from 17 to 11 carbon atoms chiral aggregates, that is, twisted fibres, were found to form (see Figure 6a, aqueous

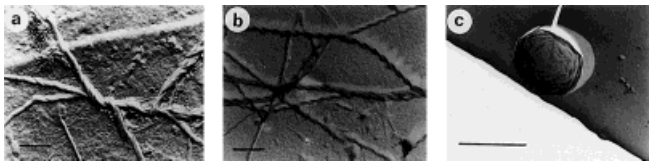

Figure 6. Electron micrographs (Pt shadowing) of a 0.1% (w/w) dispersion of a) **5b** (bar 500 nm), b) **5a** after addition of 0.25 mol equiv $CuSO_4$ (bar 200 nm), c) **5a** after addition of 0.25 mol equiv $Cu(SO_3CF_3)_2$ (bar 1 μm).

0.1% (w/w) dispersions of **5b**). These fibres all showed a right-handed twist and displayed a phase transition at 18°C. The pitch of these fibres was not very regular, probably owing to the fact that at room temperature they are in their liquid crystalline phase.

Addition of 0.25 molar equivalents of copper sulfate[22] to a 0.1% dispersion of **5a** and subsequent sonication at 70°C caused the formation of vesicles with diameters of 200–1000 nm. Upon ageing at 4°C for one day, these vesicles were transformed into right-handed helical ribbons with a regular pitch of 103 nm and a thickness of approximately 30 nm (Figure 6b). For these aggregates a bilayer thickness of 38 Å was calculated from the powder diffraction data (Table 1). This indicates that the helices are also built up from intercalated bilayers. The thickness of the ribbons could be determined from the electron micrographs; it approximated to 160 Å, suggesting that they are formed by the regular twisting of four stacked bilayers.

These helical ribbons were found to undergo a weak phase transition at 31°C, implying a decrease in the molecular organisation of the bilayers as compared to the aggregates formed from dispersions of pure **5a**. Monolayer experiments showed a larger molecular area for the copper sulfate complex of **5a** than for pure **5a** (60 and 56 $Å^2$, respectively; Table 1). This change in molecular area may be attributed to an increase in head-group size, which is consistent with the decrease in hydrocarbon chain organisation deduced from the DSC experiments.

When copper triflate was added to aqueous dispersions of **5a**, vesicles were again formed, as was observed by electron microscopy. These aggregates transformed into giant vesicles with diameters of approximately 5 μm (Figure 6c) upon standing. The bilayer thickness of these giant vesicles was 40 Å, again pointing to intercalation of the hydrocarbon chains. DSC revealed a weak phase transition at 20°C (Table 1) indicating that at room temperature the aggregates are in their liquid-crystalline phase.

The different aggregation behaviour of the triflate complexes compared to the sulfate complexes is probably due to a change in head-group size, which arises from the introduction of the more sterically demanding triflate ion. Monolayer experiments indicated that the use of aqueous subphases containing 1.0 M copper triflate instead of 1.0 M copper sulfate indeed led to an increase in molecular area from 60 to 63 $Å^2$ (Table 1). This increase in molecular area may be explained by assuming that these hydrophobic, noncoordinating ions will be located at the lipid–water interface (as opposed to the highly polar sulfate ions which will be dissolved in the aqueous phase), separating the copper complexes. This is supported by the increase in the lift-off area observed in the case of the triflate complexes, indicating that steric interactions between the amphiphilic complexes and the triflate ions already play a role in the liquid expanded (LE) phase.

FT-IR studies: FT-IR spectra of oriented films of surfactants **1**–**5** were recorded in order to investigate the role of hydrogen bonding in the aggregates. All compounds were found to form an amide polymer structure, that is, an alignment in which the amide functions were linked by hydrogen bonds in an all-*trans* fashion.[23] This was concluded from the presence of both an amide II band at 1550–1539 cm^{-1} and an amide I vibration shifted to lower wave

0947-6539/98/0401-0130 $ 17.50+.50/0 *Chem. Eur. J.* **1998**, *4*, No. 1

numbers compared to the value of 1675 cm^{-1} observed for a free amide C=O group.[24]

In order to visualise the information, assemblies of several molecules of **1**–**5** were constructed with the help of CPK models (Figure 7), taking into account the formation of amide polymer chains and the occurrence of the hydrogen bonds as deduced from the analysis of the infrared spectra.

*Compound **1***: The ester carbonyl group of **1** showed two vibrations, namely at 1731 and 1714 cm^{-1}, indicating its involvement in two different types of hydrogen bonds.[25] Deconvolution of the spectrum revealed that the amide I vibration of **1** consisted of two superimposed peaks, a sharp vibration at 1644 and a broadened one at 1645 cm^{-1}, implying that the amide carbonyl group was also involved in two different hydrogen bonds.

In spectra of dilute chloroform solutions of **1**, in which no three-dimensional aggregates are formed, only one amide I vibration at 1643 cm^{-1} was observed; however, peaks characteristic of the presence of an amide polymer were still present. This indicates that **1** generates linear strands of hydrogen-bonded molecules rather than networks in dilute solution. The disappearance of interpolymer linkages was supported by the fact that the ester carbonyl vibration at 1714 cm^{-1} had disappeared, as had a small vibration at 3535 cm^{-1}. The latter was assigned to hydrogen-bonded water molecules, which may act as linkages between neighbouring amide polymer chains, connecting ester and amide carbonyl groups in the three-dimensional aggregates.

The fact that the ester vibration is present in chloroform at 1727 cm^{-1} suggests that the carbonyl function of the ester group is involved in a relatively weak hydrogen bond with a donating moiety within the same amide polymer strand. According to CPK models a hydrogen bond between the ester carbonyl group and the amide hydrogen of the same molecule is unlikely, but a hydrogen bond with the amide hydrogen of a neighbouring molecule in the strand is feasible.[26] It is proposed that the two carbonyl groups form a double hydrogen bond with the amide proton of a neighbouring molecule (Figure 7a and Figure 8). This involvement of two

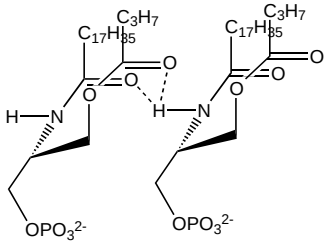

1

Figure 8. Possible hydrogen bonding pattern of **1** in chloroform solutions.

carbonyl groups may strengthen this hydrogen bond and hence account for the fact that even in dilute chloroform solutions the amide polymer structure remains present.

*Compound **2***: Two ester carbonyl vibrations were also observed for oriented films of compound **2**: one at 1737 cm^{-1}, indicative of a free ester function, and one at 1706 cm^{-1}, typical for an ester group forming a strong hydrogen bond, for example with water.[27] Considering the molecular conformation of **2** as depicted in Figure 2, this result may be explained by assuming that the ester functions are only partially hydrated after the drying procedure. The amide I signal appeared as three superimposed vibrations, a sharp peak at 1641 cm^{-1}, a broadened one at 1648 cm^{-1}, and a minor vibration at 1675 cm^{-1}. These peaks are interpreted in the following manner: a small fraction of the amide carbonyl groups is not involved in hydrogen bonding, giving rise to the weak vibration at 1675 cm^{-1}, whereas the major fraction of the amide carbonyl groups forms a (second) hydrogen bond to water molecules (1648 cm^{-1}) in addition to the aforementioned amide polymer hydrogen bond (1641 cm^{-1}). The observation of OH vibrations at 3494 and 3407 cm^{-1} supported the involvement of water molecules in hydrogen bonding to the carbonyl groups of the amide and ester functions. The OH vibrations are assigned to free water, bound to the ester carbonyl group, and crystal water possibly bridging between the amide carbonyl group and the phosphate group. The latter water molecules gave rise to a broadened P=O band at 1255 cm^{-1}.[28]

The CPK models of **2** revealed that the phosphate groups are inclined to adopt an orientation favouring the formation of an intermolecular sequence of hydrogen bonds (Figure 7b).

*Compound **3***: The appearance of two amide I vibrations in the spectrum of **3**, a sharp vibration at 1641 cm^{-1} superimposed on a broadened one at 1650 cm^{-1}, implies that also in this case the amide carbonyl group is involved in different types of hydrogen bonds. Since only one hydrogen donor is present (the amide N–H group), water molecules probably also participate as donor groups. Spectra of cast films of dispersions of **3** prepared in D_2O revealed a shift of the carbonyl vibrations to lower wave numbers. Furthermore, a change in the pattern of the phenyl ring vibrations and a broadening of the ether bands in the 1250–1200 cm^{-1} and 1060–1020 cm^{-1} regions were observed. This indicates that both the ether group and the amide carbonyl group are involved in hydrogen bonds with water. Inspection of CPK models revealed that water molecules cannot form a bridge between the amide carbonyl group and the ether oxygen atom of the same molecule. This leads to the tentative conclusion that water molecules interlink the carbonyl and phenoxy groups of neighbouring amide polymer chains.

The infrared spectra revealed that also on lowering the pH to 2.5 the amide polymer chain remained intact. An additional, broad amide I vibration appeared, which was accompanied by a broadening of the amide II vibration. The sharpening of the phenyl ring vibrations at 1600, 1580 and 1500 cm^{-1}, the appearance of a broad Ph–O ether vibration at 1222 cm^{-1} and the shift of the CH_2–O ether vibration to 1047 cm^{-1} indicated that a different hydrogen bonding pattern was formed with respect to the phenoxy group.

Since at pH 2.5 the phosphate head groups may be assumed to be fully protonated (vide infra) and hence will be less hydrated, it is likely that they can act as hydrogen donor groups to acceptor groups in the aggregate. Inspection of CPK

a

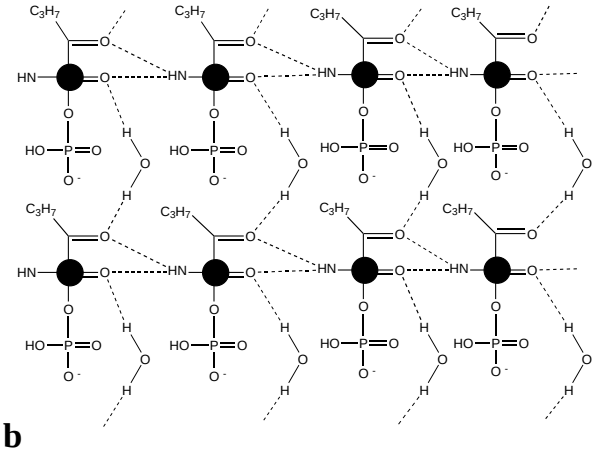

b

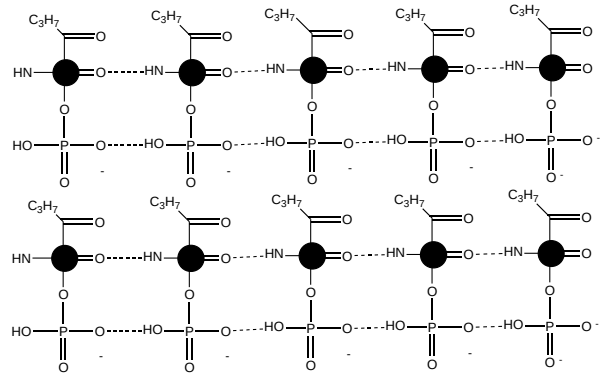

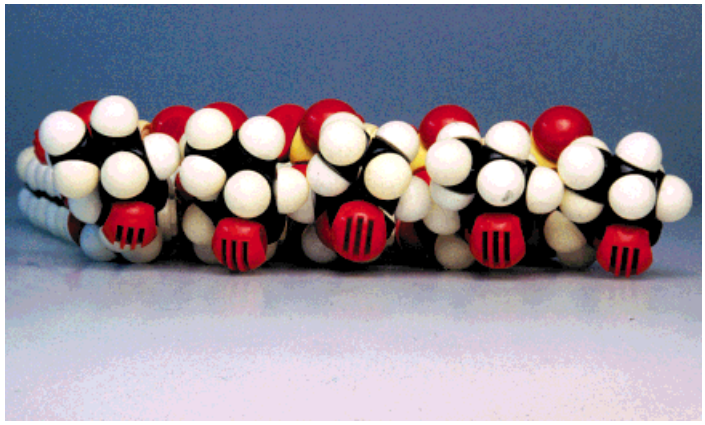

c

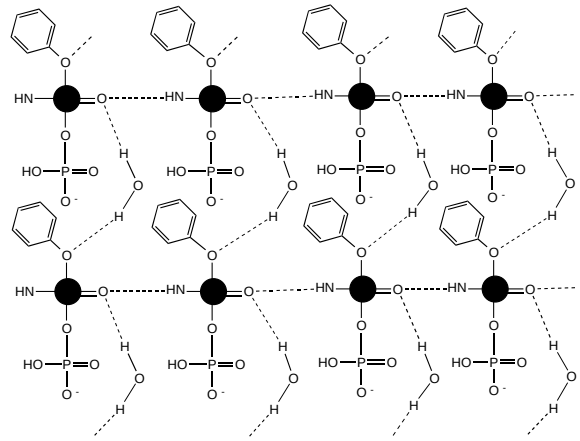

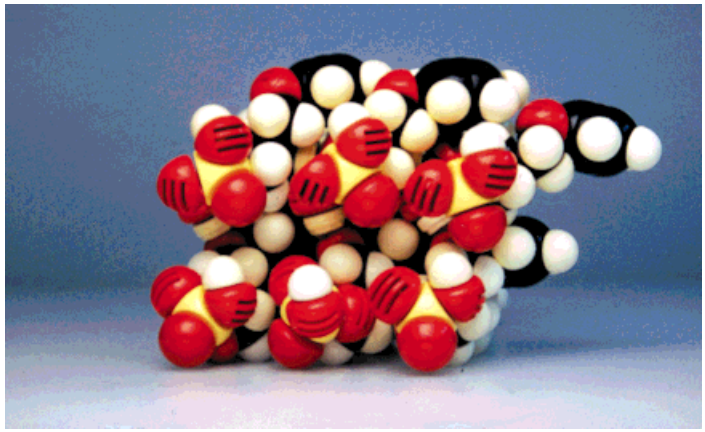

d

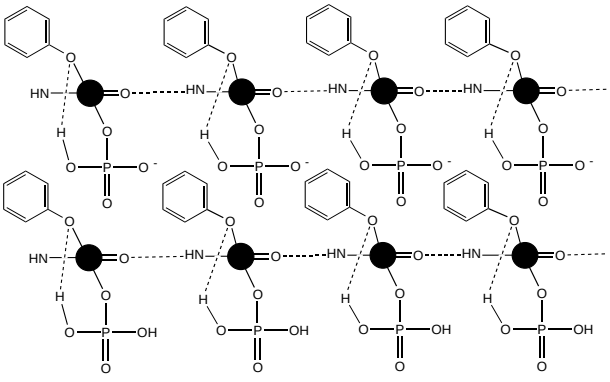

 0947-6539/98/0401-0132 $ 17.50+.50/0 *Chem. Eur. J.* **1998**, *4*, No. 1

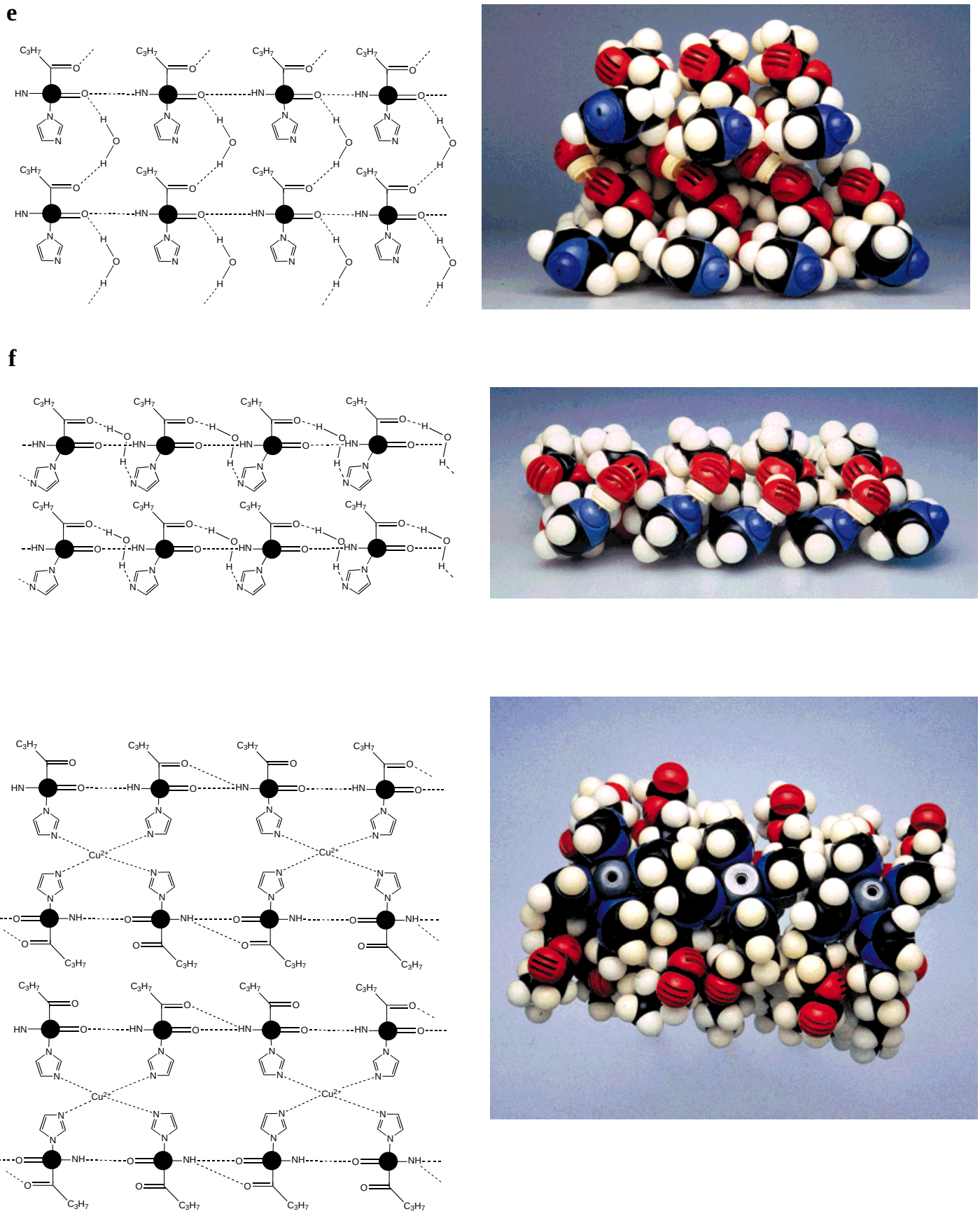

Figure 7. Schematic representations (left) and CPK models (right) showing the most probable conformations in assemblies of a) **1** at pH 6.5, b) **2** at pH 6.5, c) **3** at pH 6.5, d) **3** at pH 2.5, f) **5a** at pH 6.5, g) **5b** at pH 6.5, h) **5a** after copper(II) ion complexation. The black circles represent the parts in the molecules that are not involved in the hydrogen bonding network.

  0947-6539/98/0401-0133 $ 17.50+.25/0

models showed that no hydrogen bonds could be formed between the amide carbonyl groups and the phosphate groups without disrupting the linear amide polymer. The formation of hydrogen bonds between the phosphate groups and the ether oxygen atoms would be feasible, however, and would explain the changes in the shape and position of the ether and phenyl vibrations. Such an arrangement of hydrogen bonds would force the aromatic rings to point to the interior of the bilayer, inducing a high degree of head-group organisation, and consequently lead to a lower degree of intercalation of the hydrocarbon chains, explaining the observed increase of the bilayer thickness on changing the pH from 6.5 to 2.5 (Table 1). The proposed arrangement of the molecules of **3** at pH 6.5 and 2.5 is shown in Figure 7c and Figure 7d, respectively.

*Compound **4***: The FT-IR spectra of **4** showed a distinct broadening of the N–H stretching vibration, as well as a broadening of the amide I and the amide II vibrations, indicating that the hydrogen bonds in the amide polymer chains of **4** are less well defined than those in the aggregates of compound **3**. Furthermore, the centre of the amide I vibration appeared at a relatively high wave number, 1650 cm^{-1}, implying that the hydrogen bonds are relatively weak. IR spectra obtained from samples prepared in D_2O showed a shift of the phenyl ring vibrations, as well as a change in the pattern of the ether vibrations in the 1250–1200 and 1060–1020 cm^{-1} regions. This suggests that also in this case the phenoxy group is involved in hydrogen bonding.[29] CPK models indicated that in the case of **4** a water molecule can form a bridge between the amide carbonyl group and the phenyl ether oxygen atom. This will, however, force the phenyl ring to adopt an orientation that is sterically unfavourable for the formation of a linear amide polymer chain. A nonlinear array of hydrogen bonded amide groups may explain the broadening of the C=O and N–H vibrations in the IR spectra. It also explains why **4** forms micellar instead of lamellar structures, and would be in good agreement with the proposed staircase-like arrangement in the aggregates (Figure 5).

*Compounds **5a** and **5b***: The spectra obtained from cast films of **5a** showed a vibration at 1507 cm^{-1}, indicative of a noncoordinating imidazole group,[30] and a sharp amide I vibration at 1645 cm^{-1}. The presence of another, very broad amide I vibration at 1662 cm^{-1} suggests that the amide carbonyl group is also involved in a second, less well defined, type of hydrogen bond. The vibration of the ester carbonyl group was found at 1729 cm^{-1}, implying that this group is involved in hydrogen bonding.[31] H_2O/D_2O exchange experiments showed that in D_2O the broadened amide I vibration and the ester C=O vibration shifted to lower wave numbers, indicating that both carbonyl functions are engaged in hydrogen bonding to water molecules.[32]

CPK models revealed that the orientation of the ester carbonyl groups with respect to the amide groups is restricted in such a way that water molecules cannot bridge between ester and amide groups of the same molecule. Rather, they will interlink different amide polymers. The proposed arrangement of the molecules of **5a** is depicted in Figure 7e.

FT-IR spectra of cast films of **5b** revealed a noticeable difference in hydrogen bond formation compared to **5a**. The disappearance of the broad amide I vibration at 1662 cm^{-1} suggests that in the aggregates of **5b** water molecules no longer bind to the amide groups. The presence of an ester carbonyl vibration at 1725 cm^{-1} indicates, however, that this group is still involved in hydrogen bonding. The most striking observation, though, was the shift of the imidazole vibration to 1523 cm^{-1}, implying that this function now is involved in hydrogen bonding. It is tentatively proposed that in the aggregates of **5b** ester carbonyl groups are linked to imidazole groups by hydrogen-bonded water molecules. Inspection of CPK models of **5b** showed that a water molecule cannot span the distance between the imidazole group and the ester group of the same surfactant molecule. A connection of these groups can only be accomplished by linking two neighbouring molecules in the amide polymer. This leads to arrays of surfactant molecules forming noninterlinked polymers with highly organised head groups (Figure 7f).

*Copper complexes of **5a***: IR spectra of cast films of the copper sulfate complex of **5a** revealed that the imidazole vibration had shifted all the way to 1528 cm^{-1}, indicating that the free ligand was no longer present.[22,30] In addition to a shifted amide I vibration at 1647 cm^{-1}, a minor vibration at 1676 cm^{-1} was observed, indicating the presence of a small amount of free amide carbonyl groups. The ester carbonyl showed two equally intense vibrations, at 1726 and 1740 cm^{-1}, suggesting that these carbonyl groups are partially involved in hydrogen bonding.

According to the CPK models presented in Figure 7g, **5a** can still form linear arrays of hydrogen-bonded amide groups in the 4:1 complex with copper(II) ions. These CPK models show two different orientations for ester carbonyl groups in the copper complex, in agreement with the observation of two ester carbonyl vibrations in the infrared spectrum. This points to an only partial involvement of the ester groups in hydrogen bonding.

Although the characteristic features of the aggregates changed dramatically upon changing of the counterions of the copper(II) complex of **5a**, the FT-IR spectrum revealed a strong resemblance between the copper sulfate complex and the copper triflate complex. It may be concluded, therefore, that they have the same structure. The difference in molecular organisation is probably due to a change in head-group size, only arising from the introduction of the more sterically demanding triflate ion.

Conclusion

The experiments described above demonstrate that surfactant molecules having a strong structural resemblance can have rather different aggregation behaviour. Clearly, the formation of an amide polymer structure alone does not suffice for the formation of chiral aggregates. The CPK models constructed with the information obtained by FT-IR spectroscopy suggest that the differences in aggregation behaviour of surfactants **1**–**5** may be attributed to dissimilarities in hydrogen bonding patterns and conformational preferences. These CPK models,

0947-6539/98/0401-0134 $ 17.50+.50/0 *Chem. Eur. J.* **1998**, *4*, No. 1

shown in Figure 7, indicate that only in the case where a high degree of head-group organisation is achieved (i.e. aggregates of **2** and **5b**) can molecular chirality be expressed at the supramolecular level. The hydrogen bonding patterns in the aggregates can be altered. It was demonstrated that the resulting conformational and orientational changes can induce supramolecular chirality or can reverse the chiral patterns. CPK models also showed that in these cases the induction of supramolecular chirality is accompanied by an increase in head-group organisation (i.e., aggregates of **3** and **5a**). The presence of hydrogen-bonding water molecules which interlink the linear strands of the amide polymers seems to hamper the organisation of the head groups and thereby the supramolecular expression of chirality.

Experimental Section

The syntheses of compounds **1**–**5** have been described elsewhere,[11] as have the procedures for differential scanning calorimetry, powder diffraction and monolayer experiments.[33]

Sample preparation: Samples were prepared by sonication of a dispersion of the surfactant in water at 70 °C for 1 hour. Copper complexes were prepared by addition of the desired amount of a 1.0 mM aqueous solution of the copper salt to a sonicated dispersion of the surfactant and additional sonication for 30 min at 70 °C. Samples were aged for 16 h at room temperature prior to use, except where otherwise indicated.

Electron microscopy: Pt-shadowed samples were prepared by bringing a drop of the dispersion onto a Formvar-coated microscope grid. The excess of the dispersion was blotted off with filter paper after 1 min and the sample was shadowed under an angle of 45° by evaporation of Pt. Negatively stained samples were prepared in an analogous manner and stained with a 2% (w/w) aqueous uranyl acetate solution. Freeze-fractured samples were prepared by a Balzers freeze etching system BAF 400 D. After fracturing, the samples were etched for 1 min ($\Delta T = 20\,^{\circ}C$), shaded with Pt (angle 45°; layer thickness 2 nm) and covered with carbon (layer thickness 20 nm). All samples were studied with a Philips TEM 201 microscope (60 kV).

FT-IR spectroscopy: Films of the aggregates of **1**–**4** were prepared by depositing a surfactant dispersion on a AgCl window by the iso-potential spin drying method[35] and were studied by FT-IR absorption spectroscopy with a Mattson Cygnus 100 single-beam spectrometer equipped with a liquid-nitrogen-cooled narrow-band MCT detector. Films of **5** and their complexes were prepared by casting dispersions onto gold-coated glass supports and were studied using a Biorad STS 25 single-beam spectrometer equipped with a DTGS detector and a specular reflectance unit.

The optical bench was continuously purged with dry nitrogen gas (20 l min^{-1}). The following acquisition parameters were used: resolution 2 cm^{-1} (specular reflectance spectroscopy) and 4 cm^{-1} (absorption spectroscopy); number of co-added interferograms 128; moving mirror speed 2.53 cm s^{-1}; wave number range 4000–750; apodisation function triangle. Signal to noise ratios (2000–2200 cm^{-1}) were better than 4×10^3.

Data acquisition was performed using EXPERT-IR (Mattson) for the absorption spectroscopy experiments and WIN-IR software (Spectracalc) for the specular reflectance experiments. For data analysis WIN-IR software (Spectracalc) was used. Baselines were corrected, and peak positions were determined from second-derivative spectra smoothed over 13 data points. Curve-fitting procedures were repeated several times (initial settings 10% Gauss/90% Lorenz; bandwidth 10 cm^{-1}), and the quality of the fitted spectra was checked by comparing the generated and original spectra before and after deconvolution.

Acknowledgments: The authors would like to thank H.P.M. Geurts (Department of Electron Microscopy, University of Nijmegen) for assistance in performing electron microscopy.

Received: June 16, 1997 [F728]

[1] J. H. Fuhrhop, W. Helfrich, *Chem. Rev.* **1993**, *93*, 1565–1582, and references therein.

[2] a) K. Yamada, H. Ihara, T. Ide, T. Fukumoto, C. Hirayama, *Chem. Lett*. **1984**, 1713–1716; b) I. Sakurai, T. Karvamura, A. Dakurai, A. Kegami, T. Setoi, *Mol. Cryst. Liq. Cryst.* **1985**, *130*, 203–222; c) N. Nakashima, S. Asakuma, T. Kunitake, *J. Am. Chem. Soc*. **1985**, *107*, 509–510; d) T. Kunitake, N. Yamada, *J. Chem. Soc. Chem. Commun*. **1986**, 655–656; e) T. Kunitake, J.-M. Kim, Y. Ishikawa, *J. Chem. Soc. Perkin Trans. 2*, **1991**, 885–890; f) T. Imae, Y. Takahashi, H. Muramatsu, *J. Am. Chem. Soc*. **1992**, *114*, 3414–3415.

[3] a) H. Yanagawa, Y. Ogawa, H. Furuta, K. Tsuno, *Chem. Lett.* **1988**, 269–272; b) H. Yanagawa, Y. Ogawa, H. Furuta, K. Tsuno, *J. Am. Chem. Soc.* **1989**, *111*, 4567–4570.

[4] a) D. G. Rodes, S. L. Blechner, P. Yager, P. E. Schoen, *Chem. Phys. Lipids* **1988**, *49*, 39; b) J. M. Schnur, *Science* **1993**, *262*, 1669–1676, and references therein.

[5] a) T. A. A. Fonteijn, D. Hoekstra, J. B. F. N. Engberts, *Langmuir* **1992**, *8*, 2437; b) F. Giulieri, M. P. Krafft, *Angew. Chem.* **1994**, *106*, 1583; *Angew. Chem. Int. Ed. Engl*. **1994**, *33*, 1514; c) J. G. Riess, F. Giulieri, F. Guillod, J. Greiner, M. P. Krafft, J. G. Riess, *Chem. Eur. J.* **1996**, *2*, 1335.

[6] a) J.-H. Fuhrhop, P. Schnieder, E. Boekema, *J. Am. Chem. Soc.* **1988**, *110*, 2861–2867; b) J.-H. Fuhrhop, S. Svenson, C. Boettcher, E. Rössler, H. M. Vieth, *J. Am. Chem. Soc.* **1990**, *112*, 4307–4312; c) X. Lu, Z. Zhang, Y. Liang, *J. Chem. Soc. Chem. Commun.* **1994**, 2731–2732; d) J. M. Schnur, B. R. Ratna, J. V. Selinger, A. Singh, G. Jyothi, K. R. K. Easwaran, *Science* **1994**, *264*, 945.

[7] a) T. C. Lubensky, J. Prost, *J. Phys. II* **1992**, *2*, 371; b) W. Helfrich, J. Prost, *Phys. Rev. A* **1988**, *38*, 3065; c) P. Nelson, T. Powers, *Phys. Rev. Lett*. **1992**, *69*, 2409; d) M. S. Spector, K. R. K. Easwaran, G. Jyothi, J. V. Selinger, A. Singh, L. M. Schnur, *Phys. Rev. E* **1996**, *53*, 3804–3818.

[8] J. M. Boggs, *Biochim. Biophys. Acta* **1987**, *906*, 353.

[9] D. A. Frankel, D. F. O'Brien, *J. Am. Chem. Soc.* **1994**, *116*, 10057–10069.

[10] a) N. A. J. M. Sommerdijk, P. J. J. A. Buynsters, A. M. A. Pistorius, M. Wang, M. C. Feiters, R. J. M. Nolte, B. Zwanenburg, *J. Chem. Soc. Chem. Commun*. **1994**, 1941–1942; b) *ibid*. **1994**, 2739.

[11] N. A. J. M. Sommerdijk, P. J. J. A. Buynsters, H Akdemir, D. G. Geurts, M. C. Feiters, R. J. M. Nolte, B. Zwanenburg, *J. Org. Chem*. **1997**, *62*, 4955.

[12] This is also supported by the finding that isotherms of **1** recorded at 10, 20 and 30 °C all showed a plateau, indicating a liquid expanded (LE)–liquid condensed (LC) coexistence region. The transition pressure was temperature-independent whereas the lift-off area was strongly temperature-dependent. From these results it may be concluded tentatively that in the LE phase of **1** the molecular area is determined by the conformational motions in the hydrocarbon chains. Apparently, upon further compression this area depends only on the size of the head group. In the compressed state, then, the molecular area will be determined by the head group, which will be less influenced by thermally induced conformational motions due to intermolecular hydrogen bonding. In isotherms of **2** the transition pressure was temperature-dependent and the lift-off area temperature-independent. The molecular area in the LE phase is independent of the conformations of the alkyl chains, but in the LC phase these conformations play a major role in determining the molecular area. Changes in the head group organisation due to conformational motions of the butyrate group would explain the effect of temperature on the molecular area in the LC phase, wheras the overall shape of the molecule accounts for the observed low area per surfactant molecule.

[13] a) D. Hönig, D. Möbius, *J. Phys. Chem.* **1991**, *62*, 4590–4592; b) S. Hénon, J. Meunier, *Rev. Sci. Instrum*. **1991**, *62*, 936–939.

[14] Chiral monolayer domains were also observed during fluorescence microscopy experiments using 0.5 mol% *sn*-1,2-dipalmitoyl-3-glycerolphosphatidylethanolaminesulfurodamine. The size of these domains was drastically reduced compared to the ones observed by Brewster angle microscopy. This remarkable difference is probably due to the fluorescence probe, which acts as an impurity and causes an increase in the number of nucleation sites.

[15] The formation of more strongly curved domains at lower temperatures can be attributed to tilting of the surfactant molecules: a) D. J. Keller, H. M. McConnell, V. T. Moy, *J. Phys. Chem.* **1986**, *90*, 2310;

b) V. T. Moy, D. J. Keller, H. E. Gaub, H. M. McConnell, *ibid.* **1986**, *90*, 3198.
[16] Z. Reich, L. Zaidman, S. B. Gutman, T. Arad, A. Minski, *Biochem.* **1994**, *33*, 14177 – 14184.
[17] The approximate pK_a values of **1** and **2** were estimated from the corresponding pK^*_a values which were determined from titration experiments in a methanol/water mixture (95/5, v/v) to prevent aggregation. The obtained pK^*_{a1} values for **1** and **2** were 4.7 and 4.3, respectively. The respective pK^*_{a2} values were 11.2 and 10.9.
[18] a) R. M. Weis, H. M. McConnell, *Nature* **1984**, *310*, 47 – 49; b) C. M. Knobler, Science, **1990**, *249*, 870 – 874.
[19] The repetitive distance d_s represents the side of the cell in the hexagonal lattice in which the hydrocarbon chains are packed. This distance appears in the powder diffraction pattern of phospholipids as a reflection representing a *d* spacing of approximately 4.0 – 4.5 Å. A tilted orientation of surfactant molecules with respect to the bilayer normal generally gives rise to an asymmetric broadening of the d_s reflection. See: a) T. Gulik-Krzywicki, E. Rivas, V. Luzzati, *J. Mol. Biol.* **1967,** *27*, 303; b) A. Tardieu, V. Luzzati, *ibid*. **1973**, *75*, 711; c) J. L. Ranck, L. Mathieu, D. M. Sadler, A. Tardieu, T. Gulik-Krzywicki, V. Luzzati, *ibid.* **1974**, *85*, 249.
[20] J.-H. Fuhrhop, P. Schnieder, J. Rosenberg, E. Boekema, *J. Am. Chem. Soc.* **1987**, *109*, 3387 – 3390.
[21] The pK_a values of **3** are assumed to be similar to those of **1** and **2** (see ref. [17]).
[22] Related systems have been shown to form copper complexes of the type [Cu(imidazole)$_4$]. See: a) R. J. H. Hafkamp, M. C. Feiters, R. J. M Nolte, *Angew. Chem.* **1994**, *106*, 1054; *Angew. Chem. Int. Ed. Engl*. **1994**, *33*, 986; b) J. H. van Esch, M.Damen, M. C. Feiters, R. J. M. Nolte, *Recl. Trav. Chim. Pays-Bas* **1994**, *113*, 186 – 193.
[23] The presence of an amide II vibration at ca. 1550 cm^{-1} and two N – H stretching vibrations at ca. 3300 and 3070 cm^{-1} is characteristic of a *trans*-amide polymer structure: N. Colthup, L. Daly, S. Wiberley, *Introduction to Infrared and Raman Spectroscopy*, Academic Press, New York, **1964**, pp. 263 – 265.
[24] For **1** and **2** the N – H stretching vibrations appear as doublets, probably due to Fermi resonance, i.e. the interaction of a fundamental vibration and an overtone of similar energy and symmetry. See: J. Overend, *Infrared Spectroscopy and Molecular Structure*, Elsevier, New York, **1963**, pp. 345. This is also the case for the amide II vibration of compound **1**, which showed two bands, namely at 1562 and 1549 cm^{-1}.
[25] A free ester carbonyl group gives rise to a vibration at 1740 cm^{-1} (see ref. [23]).
[26] This interpretation is supported by the fact that a N – H stretching vibration at 3355 cm^{-1} occurs in both the spin-dried sample and in the chloroform solution.
[27] A. Blume, W. Hubner, G. Messner, *Biochem.* **1988**, *27*, 8230.
[28] In the models of **2** (Figure 7b) the bridging water molecules between the amide carbonyl and phosphate groups have been omitted for the sake of clarity.
[29] The appearance of a sharp amide I vibration suggests that the use of D_2O causes the formation of more well defined amide polymer chains. It is of interest to note that the dispersions of **4** in D_2O appeared to be more turbid than the dispersions of this compound in water. This may indicate that different types of aggregates are formed. The use of D_2O, therefore, may offer the possibility of tuning the aggregation behaviour of surfactants by changing the strength of their intermolecular interactions.
[30] J. Reedijk, *J. Inorg Chem.* **1971**, *33*, 179.
[31] A small vibration at 1743 cm^{-1} is also present, indicating that not all ester groups are involved in hydrogen bonding.
[32] No NH – ND exchange was observed for this compound.
[33] Compound **4** did not form a stable monolayer.
[34] N. A. J. M. Sommerdijk, T. H. L. Hoeks, M. Synak, M. C. Feiters, R. J. M. Nolte, B. Zwanenburg, *J. Am. Chem. Soc.* **1997**, *119*, 4338 – 4344.
[35] N. Clark, K. Rothschild, B. Simon, D. Luippold, *Biophys. J.* **1980**, *31*, 65.

0947-6539/98/0401-0136 $ 17.50+.50/0 *Chem. Eur. J.* **1998**, *4*, No. 1